



Article

Antibacterial and Cytotoxic Potential of Latex-Mediated Silver Nanoparticles Using *Tabernaemontana ventricosa*

Clarissa Marcelle Naidoo ^{1,2,*} , Yougasphree Naidoo ¹, Yaser Hassan Dewir ³ , Moganavelli Singh ¹ ,
Aliscia Nicole Daniels ¹, Johnson Lin ¹ and Ali Alsughayyir ⁴

¹ School of Life Sciences, University of KwaZulu-Natal, Westville Campus, Durban 4000, South Africa; naidoo1@ukzn.ac.za (Y.N.); singhm1@ukzn.ac.za (M.S.); alisciadaniels@gmail.com (A.N.D.); linj@ukzn.ac.za (J.L.)

² Department of Biology, School of Science and Technology, Sefako Makgatho Health Science University, Pretoria 0204, South Africa

³ Plant Production Department, College of Food and Agriculture Sciences, King Saud University, P.O. Box 2460, Riyadh 11451, Saudi Arabia; ydewir@ksu.edu.sa

⁴ Department of Plant and Soil Sciences, Mississippi State University, Starkville, MS 39762, USA; aa2942@msstate.edu

* Correspondence: naidooclarissa5@gmail.com

Abstract: The recent developments in nanotechnology have driven researchers towards the application of latex extracts for the green synthesis of silver nanoparticles (AgNPs). In this study, AgNPs were biologically synthesized using latex extracts from *Tabernaemontana ventricosa*, characterized, and their respective biological activities were assessed. Our results showed prominent silver (Ag) peaks at 410 nm confirmed by UV-vis while the elemental percentage composition ($3.89 \pm 0.16\%$) of the AgNPs was verified by EDX. The SEM and HRTEM analysis revealed spherical, ovate, and triangular AgNPs, with diameters ranging from 5.00 nm–17.50 nm; however, larger hydrodynamic diameters were revealed by NTA analysis. The FTIR spectra results displayed several peaks of bending and stretching associated with various functional groups such as alcohols, alkanes, amines, proteins, enzymes, and other biomolecules possibly responsible for the capping, reduction, and functionalization of AgNPs. In addition, the AgNPs showed strong antibacterial activity (diameter of the zone of inhibition) against *Escherichia coli* (12.67 ± 1.15 mm), *Staphylococcus aureus* (11.67 ± 0.58 mm), and *Pseudomonas aeruginosa* (11.33 ± 0.58 mm), with significant cytotoxic activity noted in the HeLa cells ($10.52 \mu\text{g/mL}$). The study confirmed the successful production of AgNPs and recommends *T. ventricosa* latex extracts as effective capping agents of nanoparticles (NPs).

Keywords: AgNPs; biosynthesis; antibacterial activity; cytotoxicity; latex; *Tabernaemontana*



Citation: Naidoo, C.M.; Naidoo, Y.; Dewir, Y.H.; Singh, M.; Daniels, A.N.; Lin, J.; Alsughayyir, A. Antibacterial and Cytotoxic Potential of Latex-Mediated Silver Nanoparticles Using *Tabernaemontana ventricosa*. *Appl. Sci.* **2023**, *13*, 11363. <https://doi.org/10.3390/app132011363>

Academic Editor: Gang Wei

Received: 24 September 2023

Revised: 14 October 2023

Accepted: 15 October 2023

Published: 16 October 2023



Copyright: © 2023 by the authors. Licensee MDPI, Basel, Switzerland. This article is an open access article distributed under the terms and conditions of the Creative Commons Attribution (CC BY) license (<https://creativecommons.org/licenses/by/4.0/>).

1. Introduction

Nanotechnology is an emerging trend in several fields such as physics, chemistry, material science, biology, and medicine [1,2]. Nanoparticles (NPs) are often preferred for certain applications due to their ideal specifications such as tiny particle size (<100 nm), high surface area to volume ratio, and complex electronic, optical, magnetic, chemical, and physical properties [2]. Studies have indicated that silver nanoparticles (AgNPs) are usually synthesized using chemical approaches that are often expensive, time-consuming, and involve toxic chemicals [3–5]. Due to the several limitations associated with the chemical production of AgNPs, researchers are largely focused on the development of “Biological or green synthesis” of NPs. The production of biosynthesized AgNPs is often favored due to their simplicity, effectiveness, reduced cost, and eco-friendly properties [2,3,6].

The efficient production of AgNPs using various biological methods, including utilizing microorganisms, plant extracts, or plant biomasses, has been intensively explored [3,6,7]. Furthermore, it has been suggested that plant extracts are easily maintained since they

do not require intra/extracellular synthesis, purification, or the maintenance of cell cultures [1,7]. Many reports have highlighted the biosynthesis of AgNPs using multiple plant extracts such as *Cymbopogon citratus* [8], *Tabernaemontana divaricate* [9,10], and *Tabernaemontana heyneana* Wall. [11]. However, most recently, latex extracts have been studied due to the presence of natural polymers, which act as a stabilizer for NPs [10]. Studies have been reported for *Jatropha curcas* [3], *Ficus sycomorus* [12], *Euphorbia nivulia* L. [13], *Hevea brasiliensis* L. [14], *Calotropis gigantea* L. [15], and *Euphorbia tirucalli* [6].

Tabernaemontana ventricosa Hochst. ex A. DC. (Apocynaceae) is a latex-bearing tree with a scattered distribution in Nigeria, Ghana, Kenya, and South Africa [16,17]. Traditionally, the leaves, stems, and latex of *T. ventricosa* are often used to reduce fever and hypertension, treat wounds, and heal sore eyes [18]. The pharmacological properties of this plant include antiamoebic, antibacterial, antileishmanial, and cytotoxic activities [17,19,20]. The latex of *T. ventricosa* contains an abundant source of alkaloids, phenolics, and proteins that may be responsible for the medicinal value of this species and the capping and stability of NPs [21].

The continuous developments in the identification of novel plant bioactive compounds have driven researchers toward the application of latex extracts and their respective compounds for the synthesis of AgNPs [1,22,23]. Currently, there are several reports on the “Green synthesis” of AgNPs using various *Tabernaemontana* species, such as *T. divaricata* [9,10] and *T. heyneana* Wall. [11]. To the best of our knowledge, no reports exist on the synthesis of AgNPs using latex from the *T. ventricosa* species. Considering the importance surrounding the synthesis of AgNPs using latex extracts, especially within the genus *Tabernaemontana*, the current investigation aimed to biologically synthesize, characterize, and evaluate the antibacterial and cytotoxicity of synthesized AgNPs using latex from *T. ventricosa*.

2. Materials and Methods

2.1. Latex Collection and Preparation

Plants of *Tabernaemontana ventricosa* were procured from the Westville campus of the University of KwaZulu-Natal, situated in South Africa at the coordinates 29°49′03.3″ S 30°56′32.7″ E. The aseptic collection of fresh milky white latex exudates was accomplished by severing the soft green stems, which were then carefully preserved in sterile tubes. Subsequently, the latex was diluted to a concentration of 1% by adding 1 mL to 100 mL of sterile distilled water and stored at −8 °C for future utilization.

2.2. Synthesis of AgNPs

The AgNPs were synthesized with a modified experimental analysis [12]. Approximately 90 mL of a 1 mM aqueous solution of silver nitrate (AgNO₃) (Biolab, Merck, Johannesburg, South Africa) was incrementally introduced to 10 mL latex (Lx) extract. The solution was agitated and subjected to a temperature of 80 °C for 3 h. The negative control, comprising 10 mL of distilled water and 90 mL of AgNO₃, underwent the same treatment. All analyses were replicated three times ($n = 3$).

2.3. UV-Visible Spectral Analysis

The utilization of latex extracts for the synthesis of AgNPs was verified through the application of UV-vis spectroscopy (SHIMADZU UV-1800, Duisburg, Germany) within the wavelength range of 200–800 nm. For analysis, an approximate volume of 1 mL of AgNP solution was employed, with the AgNO₃ solution acting as a reference. The resultant AgNP solution and the control were simultaneously subjected to analysis, and the corresponding optical densities (OD) were duly recorded.

2.4. Preparation, Purification, and Quantification of Samples

Following the confirmation of the synthesis of the AgNPs, the solutions underwent the processes of centrifugation, purification, and quantification. The synthesized solutions were subjected to centrifugation at a speed of 10,000 revolutions per minute (rpm) for 30 min at

a temperature of 4 °C, utilizing the BECKMAN COULTER Avanti®J-E, Indianapolis, IN, USA centrifuge, which originates from the United States of America. After each centrifugation step, the supernatants were discarded, and the remaining pellet was rinsed with 20 milliliters (mL) of distilled water. This centrifugation and wash process was performed three times to ensure the thorough removal of any additional residues. Subsequently, the final solutions were dried in an oven maintained at a temperature of 30 °C for 7 days, and the yield, specifically the dry mass, was determined. For further analyses, the dried silver nanoparticles (AgNPs) were reconstituted using sterile distilled water.

2.5. Characterization of AgNPs

2.5.1. Scanning Electron Microscopy (SEM) and Energy-Dispersive X-ray (EDX) Analysis

Scanning Electron Microscopy and Energy-Dispersive X-ray analysis were utilized for the initial characterization of synthesized AgNPs employing latex extracts. Before the analysis, the samples underwent a 20 min sonication process utilizing a SONICLEAN device from Thebarton, Australia. Subsequently, the samples were directly placed onto separate aluminum stubs and briefly dried. The stubs were then coated with a thin layer (approximately 25 nm) of gold using a sputter coater (Quorum 150 R ES, Laughton, UK). The coated samples were examined utilizing an Ultra Plus FEGSEM instrument from Carl Zeiss, Jena, Germany, operating at a voltage of 5 kV. The software used to determine the NP size, shape, and distribution was SmartSEM version 5, also from Carl Zeiss, Jena, Germany. Synchronized EDX analyses were conducted using the Zeiss Ultra Plus X-ray spectrometer, equipped with an Astronomical Thermal Emission Camera (Aztec) version 1.2, operating at 20 kV. Subsequently, the elemental composition of the samples was verified using the Aztec Analysis Software (version 1.2) from Oxford Instruments, Abingdon, UK.

2.5.2. High-Resolution Transmission Electron Microscopy (HRTEM) analysis

High-Resolution Transmission Electron Microscopy was employed to acquire highly magnified images of the morphology and size of the synthesized AgNPs. Before the analysis, a drop of sonicated AgNP latex samples was carefully deposited onto carbon-coated (Quorum Q150 TE, Laughton, UK) formvar grids (200 mesh) and subsequently dried. Following this, the samples were observed utilizing the HRTEM JEM 2100 (JEOL, Tokyo, Japan), which was equipped with Gatan software (version 3.5), operating at a voltage of 200 kV. The morphology and size of the AgNPs were ascertained through the utilization of ImageJ software (Java version 1.8.0) ($n = 5$).

2.5.3. Fourier Transform Infrared (FTIR) Spectral Analysis

Fourier transform infrared spectroscopy was employed to analyze the synthesized AgNPs using latex. The analysis was carried out using an Agilent Cary 60 spectrometer equipped with Agilent MicroLab PC version 5.1.22 software. This method aimed to investigate and categorize the surface chemistry and functional groups of the capping agents. To collect the data, an ATR Diamond-1 Bounce with 30 background and sampling scans was utilized in the range of 4000–650 cm^{-1} , with a resolution of 4 cm^{-1} . The bond patterns and peaks were identified utilizing ResolutionPro version 5.0.0.395.

2.5.4. Nanoparticle Tracking Analysis (NTA)

The size distribution and zeta potential of the AgNPs were evaluated through the utilization of the NTA technique, specifically employing the Nanosight NS500 instrument from the United Kingdom. To conduct the analysis, a 1 mL solution of 1:100 dilutions was prepared using 18 MOhm water. Subsequently, the solution was subjected to vortexing using the VM-1000 apparatus from Taipei, Taiwan, followed by sonication using the SONICLEAN device from Thebarton, Australia. These preparatory steps were undertaken before the commencement of the analyses. All measurements were executed at a temperature of 25 °C, utilizing a voltage of 24 V. The acquired images were then captured and subjected to examination utilizing the NTA version 3.2 analytical software.

2.6. Biological Assessment of Synthesized AgNPs

Sample Preparation

Stock solutions of the latex extract synthesized AgNPs using latex were prepared by suspending 1 mg of the dried AgNP powder in 1 mL of sterile distilled water. The diverse stock solutions (1 mg per mL) for the treatments were mixed thoroughly using a vortex (Model: VM-1000, Taipei, Taiwan), and reconstituted in distilled water to yield concentrations ranging from 3.125, 6.25, 12.5, 25, 50, to 100 mg per mL.

2.7. Antibacterial Screening

Various concentrations of the synthesized AgNPs using latex extracts (prepared with distilled water) were screened for antibacterial activity against three Gram-positive bacterial strains *Bacillus subtilis* (ATCC 6653), Methicillin-resistant *Staphylococcus aureus* (MRSA) (ATCC 43300), *Staphylococcus aureus* (ATCC 29213), and two Gram-negative bacterial strains *Escherichia coli* (ATCC 25922) and *Pseudomonas aeruginosa* (ATCC 27853).

The agar disc diffusion technique, recommended by the Clinical and Laboratory Standards Institute [24], was employed to determine the in vitro antibacterial screening of latex and AgNP samples. After preparing sterile Whatman filter paper No. 1, approximately 20 µL of the respective AgNP concentrations (3.125, 6.25, 12.5, 25, 50, and 100 mg/mL) were applied and allowed to dry at room temperature [25]. The bacterial strains were cultured aseptically (37 °C) for 24 h using Mueller–Hinton (MH) agar media (Biolab, Merck, Darmstadt, Germany). Subsequently, the bacteria were resuspended in sterile distilled water and vortexed (Model: VM-1000, Taiwan). The optical density (OD) of the bacterial strains (OD 0.08–0.1 at λ 625 nm) was determined using a UV-vis spectrophotometer (Agilent Technologies Cary 60 spectrophotometer, Santa Clara, CA, USA).

The inoculum was streaked across the four quadrants of the agar medium, and subsequently, the prepared discs containing samples of latex AgNPs were meticulously positioned onto the agar surface using aseptic forceps. The Petri dishes were then incubated at a temperature of 37 °C for a duration of 18–24 h, following which the zones of growth inhibition were carefully examined to ascertain the antibacterial efficacy of the AgNPs through the utilization of latex extracts. The experiment was replicated three times, with streptomycin (for Gram-positive bacteria) and gentamicin (for Gram-negative bacteria) being employed as the standard positive controls for antibacterial activity, while sterile distilled water was employed as the negative control. Additionally, the AgNO₃ solution (1 mM) was also subjected to testing. The diameter of the zone of inhibition was quantitatively measured in millimeters, the resultant data were recorded and averaged, and visual representations of the Petri dishes were captured.

2.8. MTT Cytotoxicity Assay

The present study obtained three different human cell lines, namely embryonic kidney (HEK293), breast adenocarcinoma (MCF-7), and cervical carcinoma (HeLa), from the ATCC located in Manassas, VA, USA. These cell lines were cultured in 25 cm² tissue culture flasks until they reached confluence. The culture medium used for this purpose was Eagle's Minimum Essential Medium (EMEM), supplemented with 10% (*v/v*) gamma-irradiated FBS and 1% Penicillin-Streptomycin mixture. The cells were incubated in a HEPA Class 100 Steri-Cult CO₂ incubator manufactured by Thermo-electron Corporation, USA, at a temperature of 37 °C in an atmosphere containing 5% CO₂. Upon reaching confluence, the cells were trypsinized, transferred to clear 96-well plates, and incubated at 37 °C for 24 h to promote cell adhesion. Subsequently, the cells were provided with fresh complete growth medium (EMEM + 10% FBS + 1% Penicillin-Streptomycin mixture). To conduct cell treatment, different concentrations of latex AgNP samples, approximately 100 µL, were added to the cells, followed by incubation at 37 °C for 48 h. Control cells that were not subjected to any treatment were utilized as the affirmative control, showcasing a viability of approximately 100%. The entirety of the experiments was performed in triplicate.

The methods briefly described by Mosmann [26] and Daniels and Singh [27], were used to assess the cytotoxic potential activity of the latex-synthesized AgNPs on the cell lines. After 48 h of incubation at 37 °C, the growth medium was aspirated and replaced with 100 µL of medium containing 10 µL of MTT solution (5 mg/mL in PBS), and the cells containing the treatment and negative control were incubated for a further 4 h at 37 °C in 5% CO₂. The medium-MTT mixture was then removed and replaced with 100 µL dimethylsulphoxide (DMSO). The absorbances were then determined at 570 nm using a Mindray MR-96A microplate reader (Vacutec, Hamburg, Germany). Graphs were used to determine the concentration at which 50% cell growth inhibition (IC₅₀) occurred. Percentage cell survival was calculated following the equation below.

$$\% \text{ Cell survival} = \frac{(\text{Average optical density of control cells only})}{(\text{Average optical density of treated cells})} \times 100$$

2.9. Statistical Analyses

The mean values were reported along with their corresponding standard deviations, with a sample size of three ($n = 3$). Statistical analysis was conducted utilizing the R Statistical computing software developed by the R Core Team in the year 2020, specifically version 3.6.3. Following this, Tukey's honest significant difference range post hoc tests were performed to assess statistical significance (* $p < 0.05$; ** $p < 0.01$). Visual representations were created using Microsoft Excel, version 2019.

3. Results and Discussion

3.1. Visual Inspection, UV-Visible Spectroscopy, and Quantification of Synthesized AgNPs

The synthesis of AgNPs using 1% latex extract was indicated by a slight color change. Initially, the mixture (1% latex + AgNO₃) appeared white (Figure 1A); however, following the incubation period, a light greyish color was observed (Figure 1B). Rathnayake et al. [28], reported a similar color change for the green synthesis of AgNPs inside centrifuged natural rubber latex. These visible color changes are usually related to the reduction in silver (Ag) ions by the capping of biomolecules present within the respective extracts [5,28]. Moreover, the literature has often associated a rapid and extreme color change with the production of AgNPs; however, this may vary based on several factors such as plant organ type, solvent/extract, concentration, duration of incubation, and the presence of reducing agents [29,30]. Moreover, according to studies, it appears that the concentration (%) of the latex largely influences the production of AgNPs, since Bar et al. [3] reported that a 2% latex solution was insufficient for AgNP synthesis compared to a 3% latex solution, which displayed optimal results during the green synthesis.

Coupled with the visual assessment, the formation, distribution, and stability of the synthesized AgNPs using latex was further confirmed using UV-visible spectroscopy. The analysis showed prominent silver surface plasmon resonance (SPR) bands at 410 nm with an absorbance of 0.947 (Figure 2). The wavelength of the AgNPs fell within the accepted range, which is often detected between 400 nm and 460 nm [31]. Similarly, Chandrasekaran et al. [5], displayed broad SPR peaks at 410 nm due to the collective oscillations of electrons; however, the absorbances were much higher, possibly related to the longer reaction times (72 h).

The yield of synthesized AgNPs using latex extracts amounted to 14.80%, which is a moderate quantity of AgNPs (Table 1). It was noted that several studies used higher concentrations of latex, increased temperature, and incubation times, and most importantly, each latex-bearing species contained a variable chemical composition comparable to the current study [3,32–36]. Several of the above-mentioned variables may likely influence the quantification of AgNPs.

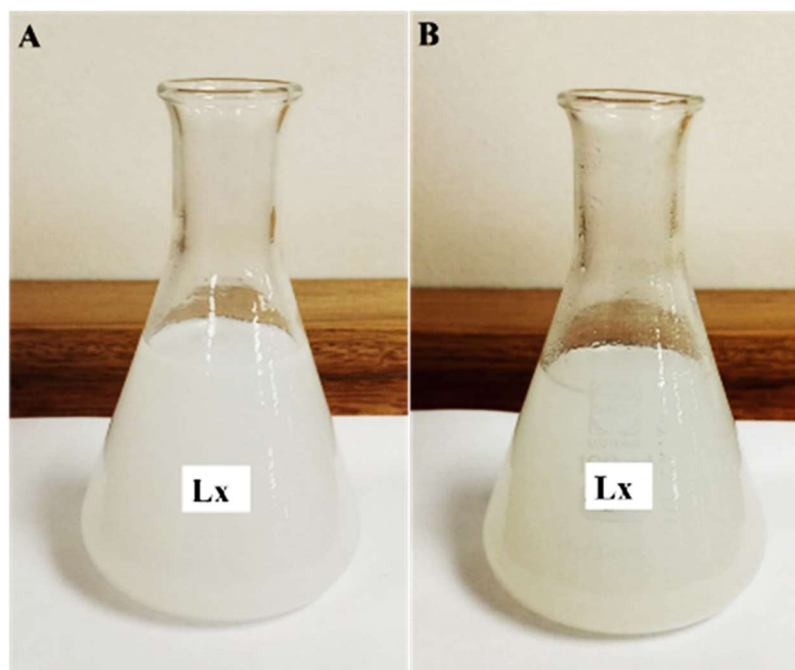


Figure 1. (A) Visual representation of latex extract + AgNO_3 before Ag nanoparticle synthesis (incubation); (B) synthesized Ag nanoparticles using latex extracts after incubation with AgNO_3 for 3 h at 80°C .

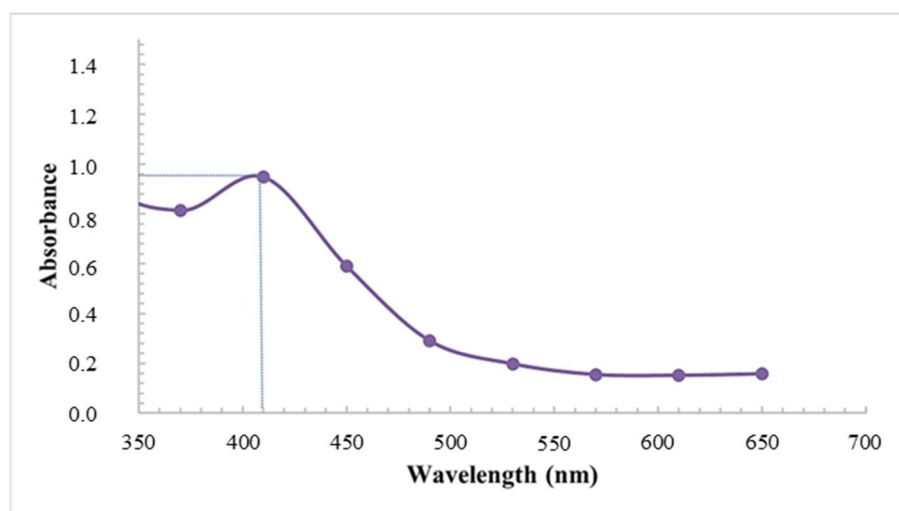


Figure 2. UV-vis spectra of AgNPs synthesized using latex extracts of *T. ventricosa*.

Table 1. The percentage yield of the synthesized AgNPs using latex extracts from *T. ventricosa*.

Extract	Latex
Dried extract yield (g)	0.15
Yield (%)	14.80

3.2. Scanning Electron Microscopy (SEM) and Energy-Dispersive X-ray (EDX) Analysis

Scanning Electron Microscopy is often employed to deduce the size and morphology of NPs, whereas the detection, confirmation, and composition of AgNPs are conducted using EDX analysis [37–39]. The SEM analysis in the present study revealed that AgNPs produced using latex extracts from *T. ventricosa* appeared <100 nm in size, mostly spherical

and extremely agglomerated as displayed in Figure 3A. These results are consistent with Borase et al. [39]. In their study, *Ficus carica* latex extracts were similarly used to produce Ag-NPs, which were mainly spherical and ranged from 50 to 200 nm; however, no occurrences of agglomeration were noted [39]. The various types of microscopes (SEM vs. ESEM), TEM, and the sample preparation techniques before analyses differ, which may account for these observable differences in agglomeration. Moreover, additional reports have shown that the variation in agglomeration may be dependent upon several other aspects such as variations in the reaction temperature, extract concentration, and AgNO₃ concentration [40,41]. Furthermore, Durgawale et al. [42] observed that the various interactions between hydrogen bonds and electrostatic forces of the bio-organic capping molecules may also influence the accumulation of smaller particle sizes, thus leading to an increased agglomeration of AgNPs.

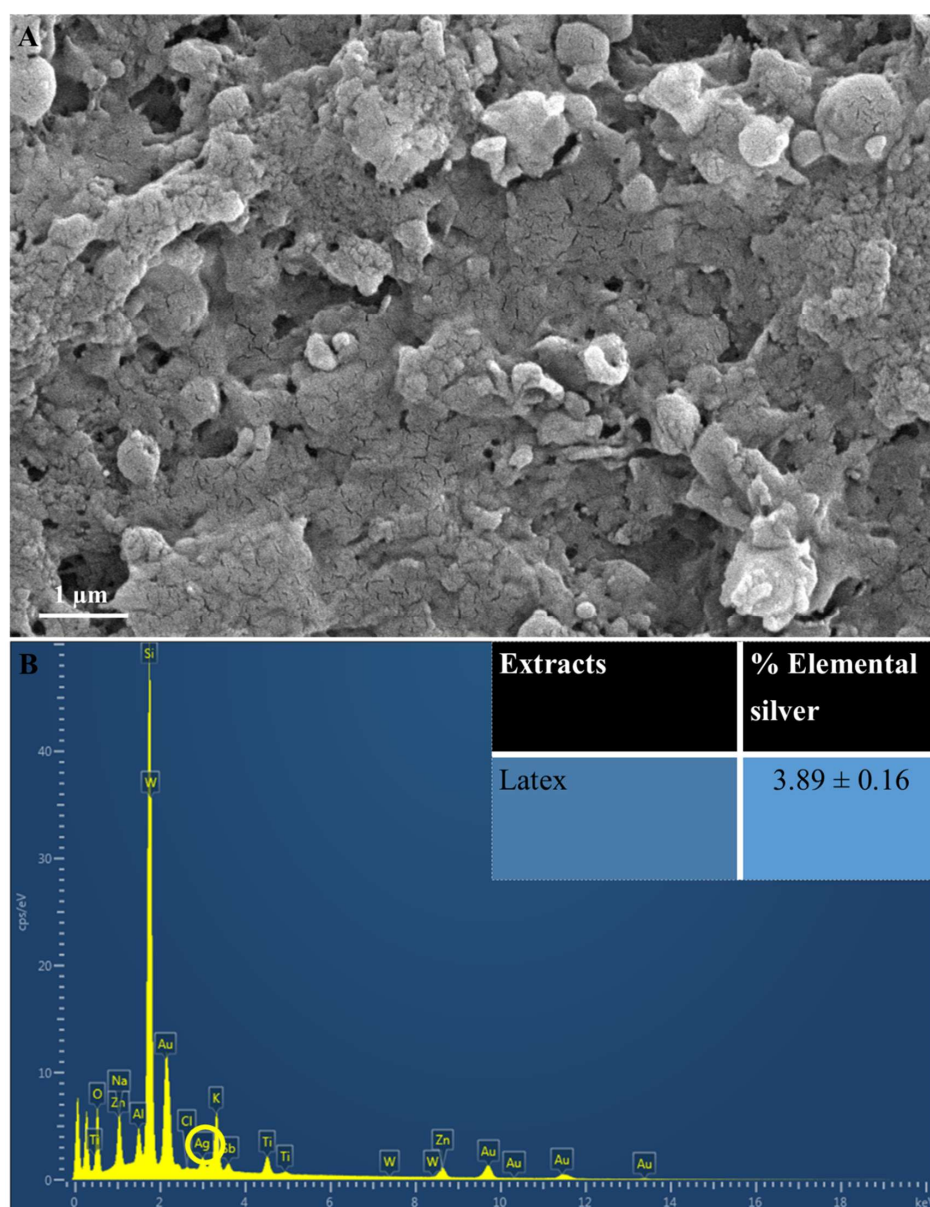


Figure 3. (A) Scanning Electron Microscopy images of AgNPs synthesized using latex extracts of *T. ventricosa*. Distinctive agglomeration within the image. (B) An EDX spectra and average elemental composition (%) of Ag in latex extracts. Circle indicated Ag.

The elemental analysis (Figure 3B) indicated the presence of elemental Ag in AgNPs synthesized using latex. The EDX spectra showed a moderate Ag peak at 3 KeV (Figure 3B), which is often associated with the optical absorption peaks of surface plasmon resonance for Ag [3,43]. Furthermore, these AgNPs displayed a percentage of elemental Ag of $3.89 \pm 0.16\%$ (Figure 3). Although the composition of elemental Ag does not appear high, the EDX analysis does confirm adequate Ag production. It has been proposed by several researchers that the observable differences in the percentage composition of AgNPs are primarily affected by the chemical composition of the bioactive compounds of various extracts [29,33,41]. Furthermore, the lower concentration of latex (1%) used in the current study may be a contributing factor, since other studies have used higher concentrations of latex for the synthesis of AgNPs [6,12,35]. Salem et al. [12] utilized 3% latex solutions from *Ficus sycomorus* for the synthesis of AgNPs, and their results revealed a yield of 98.49%, which was significantly larger compared to the current study. The occurrences of other elemental signals such as oxygen (O₂), sodium (Na), potassium (K), and various other elements (Figure 3B) are possibly due to the presence of several enzymes and proteins detected within the latex of *T. ventricosa* [3,12,33,40].

3.3. High-Resolution Transmission Electron Microscopy (HRTEM)

The HRTEM images of AgNPs synthesized using latex extracts of *T. ventricosa* are displayed in Figure 4A, whereas the particle size distribution is shown in Figure 4B. The morphological distribution of the AgNPs highlighted in Figure 4A reveals the absence of agglomeration, which is indicative that the synthesized AgNPs had good stability and were well dispersed (monodispersed) in the solution [35,44,45]. The thin matrix layer observed around the NPs is most likely due to the presence of biomolecules from *T. ventricosa* latex during the synthesis of the AgNPs, which provided further stability and prevented the formation of aggregates in the solution [1,5]. The particles appeared spherical and ovate, and some were triangular (Figure 4A). According to Bakar et al. [46], natural rubber AgNPs' characteristic features are spherical to ovate shapes. However, Duragawale et al. [42] investigated the AgNPs using latex of *Syandenum grantii* Hook F. and reported various morphologies of NPs such as spherical triangles, truncate triangles, and decahedral shapes. Many researchers have observed that NPs synthesized using latex extracts are often spherical [47–50]. The HRTEM analysis in the present study (Figure 4A) is consistent with these reports.

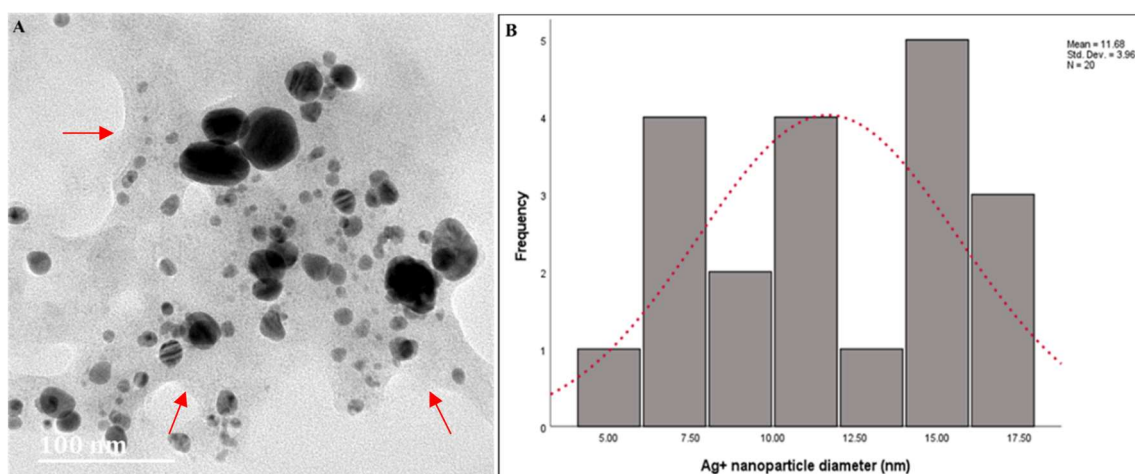


Figure 4. (A) High-Resolution Transmission Electron Microscopy micrographs of AgNPs synthesized using latex extracts from *T. ventricosa*. Arrows indicate film surrounding NPs. (B) Particle size (nm) of AgNPs synthesized using latex extracts from *T. ventricosa*. $n = 20$.

The particle size distribution obtained by Image J analysis showed an average diameter of 11.68 ± 3.96 nm, which ranged from 5.00 nm to 17.50 nm (Figure 4B). In addition, we noticed two broad size distributions of the particles, one displaying smaller diameters ranging from 5 nm to 7.50 nm, and other particles with larger diameters, ranging from 15 nm to 17.50 nm. Bar et al. [3] observed a similar occurrence, which was supported by UV-vis spectra analyses, which displayed two Ag peaks (425 nm and 464 nm). However, unlike the present study, we had only observed one Ag peak at 410 nm. The differences in the composition and concentration of extracts may be accountable for these variations [6,12,35,45]. Overall, despite the variations observed in the present study, the diameters of the AgNPs are similar to those of Bar et al. [3], Guidelli et al. [14], and Almeida et al. [35].

3.4. Nanoparticle Tracking Analysis (NTA) and Zeta Potential

The NTA analysis revealed an average diameter of 57.2 ± 5.7 nm for AgNPs synthesized using latex extracts (Table 2). Although this value may seem large, it is relatively smaller in comparison to studies where the size of particles ranged from 32 nm to 220 nm in diameter [38,39]. Furthermore, it was observed that the average diameter of particles observed using NTA analysis was much larger in comparison to HRTEM studies. It is suggested that the various techniques involved before or during analyses may influence the particle size differently. The measurement of particle size using NTA analyses in a hydrodynamic environment is often preferred since it is closely associated with an in vivo system, unlike HRTEM samples, which are in a dehydrated or powdered state [51,52].

Table 2. Average nanoparticle diameter (nm) and zeta potential (mV) of the synthesized AgNPs using latex extracts of *T. ventricosa*.

Extracts	Nanoparticle Diameter (nm)	Zeta Potential (mV)
Fresh latex extract	57.2 ± 5.7	12.3 ± 1.2

Values presented are mean \pm standard error ($n = 3$).

The zeta potential value is often used to measure the surface charges of particles to ensure their stability within colloidal solutions [39]. The zeta potential value herein was poor (12.3 ± 1.2 mV), with the preferred range being greater than 25 mV or less than -30 mV [27]. These results indicated that the latex AgNPs of *T. ventricosa* displayed poor stability, low mobility, and reduced electrostatic repulsion. Borase et al. [39] observed a zeta potential of -19.3 mV, thus suggesting moderate stability of the NPs, whereas Patil et al. [38] revealed a zeta potential of -25.2 mV. Kumar and Yadav [53] suggested that proteins, polyphenols, and carbohydrates largely influence the synthesis of NPs, which may affect the zeta potential.

3.5. Fourier Transform Infrared (FTIR) Spectroscopy

Fourier transform infrared spectroscopy measurements were calculated for AgNPs synthesized from *T. ventricosa* latex extracts to examine the interactions between the biomolecules (capping agents) within the sample extract and the synthesized NPs. The spectral assignments of AgNPs using latex extracts are displayed in Table 3, whereas the absorption peaks displaying various stretching and bending are shown in Figure 5. Prominent peaks located at 3338.07 cm^{-1} and 3283.60 cm^{-1} are assigned to alcohols [46,54]. Whereas peaks of 2924.93 cm^{-1} , 2330.92 cm^{-1} , and 2116.69 cm^{-1} were due to alkanes, carbon dioxide, and alkynes, respectively [6,54]. Remarkably, the compound classes isothiocyanate ($\text{N}=\text{C}=\text{S}$) and aromatic compounds ($\text{C}-\text{H}$) were linked to the peaks 2087.22 cm^{-1} and 1892.32 cm^{-1} [45,55]. Strong stretching of $\text{C}=\text{O}$ groups and medium bending of $\text{C}=\text{O}$ groups assigned to aldehydes and alkenes were associated with peaks of 1732.58 cm^{-1} and 1634.27 cm^{-1} , respectively [46]. Peaks at 1539.09 cm^{-1} , 1361.45 cm^{-1} , and 1336.41 cm^{-1} arise due to strong and medium bending and stretching of nitro compounds, phenols, and sulfonates [39,54]. Strong $\text{C}-\text{O}$ stretching of peaks at 1242.12 cm^{-1} , 1147.68 cm^{-1} , 1095.34 cm^{-1} were assigned to alkyl aryl ether, tertiary alcohols, and secondary alcohols,

while peaks at 1024.62 cm^{-1} and 823.30 cm^{-1} were due to the presence of amines (proteins/enzymes) and 1,2,3-trisubstituted compounds [54,56]. These results confirm the presence of several functional groups in the latex extracts and indicate that the proteins, enzymes, and other biomolecules detected within the latex allow for the capping, reduction, and functionalization of AgNPs [5,42].

Table 3. FTIR spectral assignments of synthesized AgNPs using latex extracts of *T. ventricosa*.

Absorption Frequency (cm^{-1})	Types of Absorption/Vibration	Appearance	Interference/Functional Group	Compound Class
3338.07	Stretch	Strong broad	O–H	Alcohol
3283.60	Stretch	Strong broad	O–H	Alcohol
2924.93	Stretch	Medium	C–H	Alkane
2330.92	Stretch	Strong	O=C=O	Carbon dioxide
2116.69	Stretch	Weak	C \equiv C	Alkyne
2087.22	Stretch	Strong	N=C=S	Isothiocyanate
1892.32	Bending	Weak	C–H	Aromatic compound
1732.58	Stretch	Strong	C=O	Aldehyde
1634.27	Bending	Medium	C=C	Alkene
1539.09	Stretch	Strong	N–O	Nitro compound
1361.45	Bending	Medium	O–H	Phenol
1336.41	Stretch	Strong	S=O	Sulfonate
1242.12	Stretch	Strong	C–O	Alkyl aryl ether
1147.68	Stretch	Strong	C–O	Tertiary alcohol
1095.34	Stretch	Strong	C–O	Secondary alcohol
1024.62	Stretch	Medium	C–N	Amine
823.30	Bending	Strong	C–H	1,2,3-trisubstituted

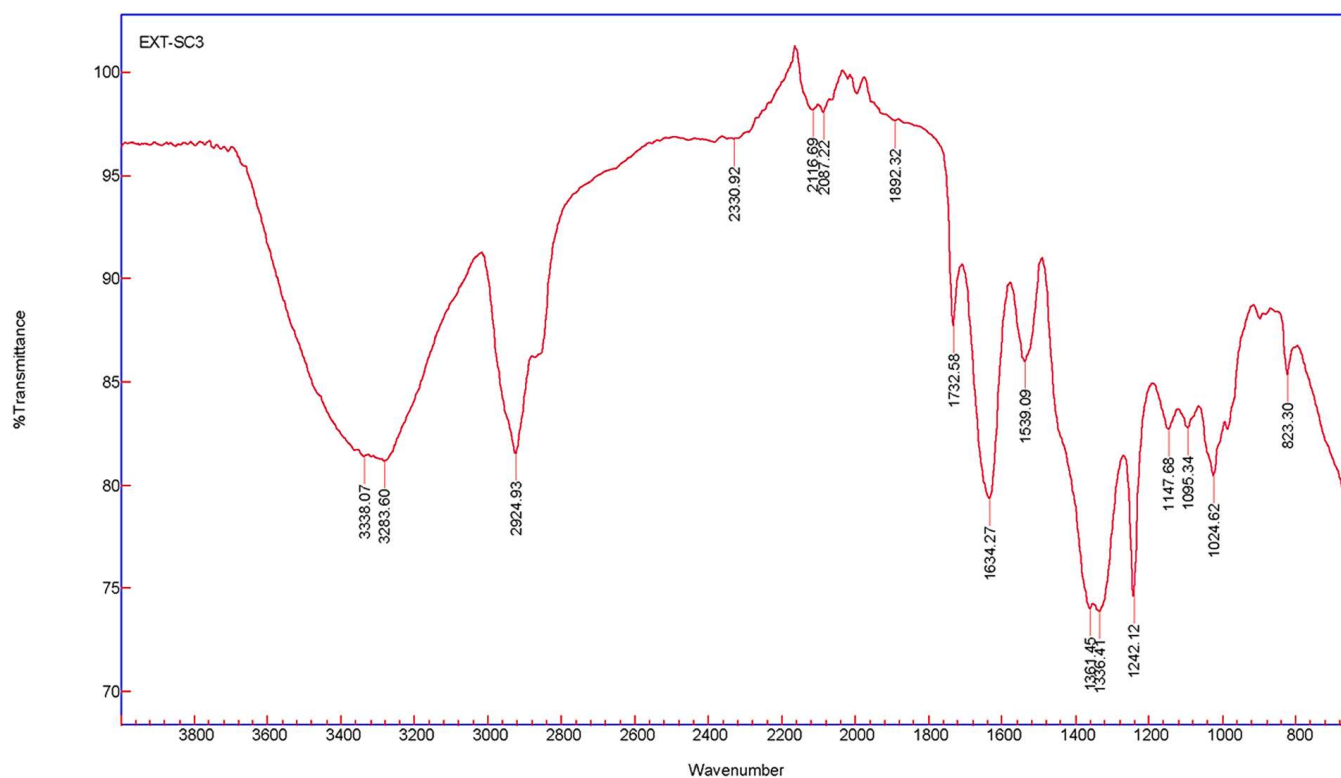


Figure 5. The FTIR spectra of AgNPs were synthesized using latex extracts of *T. ventricosa*.

3.6. Antibacterial Assay

The latex of several medicinal plants has often been utilized due to their antibacterial activities [4,6,39], and coupled with the antibacterial properties of NPs, we would expect remarkable antibacterial activity for these synthesized AgNPs using latex. Chandrasekaran et al. [5] investigated the efficiency of AgNPs using latex from *Carica papaya*, which showed significant activity against *B. subtilis*, *Enterococcus faecalis*, *E. coli*, *Vibrio cholerae*, *Klebsiella pneumoniae*, and *Proteus mirabilis*. However, despite these significant results, there appears to be a lack of interest surrounding the synthesis and antibacterial applications of AgNPs synthesized using latex extracts. Thus, one of the aims of the present study was to evaluate the antibacterial activity of latex AgNPs using agar disc diffusion. The antibacterial activity of latex AgNPs was assessed against five pathogenic bacterial strains, three Gram-positive, namely, *B. subtilis* (ATCC 6653), MRSA (ATCC 43300), and *S. aureus* (ATCC 29213), and two Gram-negative bacterial strains, *E. coli* (ATCC 25922) and *P. aeruginosa* (ATCC 27853), using a range of concentrations (3.125 to 100 mg/mL) (Table 4).

Table 4. Diameter of zone of inhibition (mm) of synthesized AgNPs using latex extracts of *T. ventricosa* against Gram-positive and Gram-negative bacterial strains.

Concentration (mg/mL)		Bacterial Strains				
		BS	EC	MRSA	SA	PA
Latex AgNPs	3.125	6.33 ± 0.58	8.67 ± 0.58	9.67 ± 0.58	9.00 ± 1.00	8.67 ± 1.15
	6.25	7.00 ± 0.00	9.00 ± 1.00	10.33 ± 0.58	10.00 ± 1.00	9.00 ± 1.00
	12.5	8.67 ± 0.58	10.67 ± 1.15	10.67 ± 1.15	10.33 ± 0.58	9.33 ± 1.15
	25	8.67 ± 0.58	11.00 ± 0.00	11.00 ± 1.00	10.67 ± 0.58	10.67 ± 0.58
	50	9.33 ± 0.58	12.33 ± 0.58	11.00 ± 1.00	11.33 ± 0.58	11.33 ± 0.58
	100	10.33 ± 0.58	12.67 ± 1.15	11.33 ± 0.58	11.67 ± 0.58	11.33 ± 1.15
Positive control (10 µg/mL)		9.67 ± 1.53 *	9.67 ± 0.58	9.33 ± 1.53 *	10.67 ± 1.15 *	9.00 ± 1.00

BS = *Bacillus subtilis* (ATCC 6653), EC = *Escherichia coli* (ATCC 25922), MRSA = *Methicillin Resistant Staphylococcus aureus* (ATCC 43300), SA = *Staphylococcus aureus* (ATCC 29213), PA = *Pseudomonas aeruginosa* (ATCC 27853), Positive controls (Gentamicin 10 µg/mL, Streptomycin 10 µg/mL *) and ($n = 3$).

The results displayed in Table 4 and Figure 6 reveal that at the lowest concentrations (3.125 mg/mL), AgNPs synthesized using latex extracts displayed minimal antibacterial activity against MRSA (9.67 ± 0.58 mm), *S. aureus* (9.00 ± 1.00 mm), *E. coli* (8.67 ± 0.58 mm), *P. aeruginosa* (8.67 ± 1.15 mm), and *B. subtilis* (6.33 ± 0.58 mm), respectively. Whereas, at higher concentrations (100 mg/mL), effective antibacterial activity was observed against *E. coli* (12.67 ± 1.15 mm), *S. aureus* (11.67 ± 0.58 mm), MRSA (11.33 ± 0.58 mm), *P. aeruginosa* (11.33 ± 0.58 mm), and *B. subtilis* (9.33 ± 0.58 mm), respectively. It was noted that the increased concentrations of latex AgNPs influenced the zones of inhibition (inhibition of bacterial growth) progressively, similar results were reported by Chandrasekaran et al. [5]. Furthermore, the results showed a substantial difference between the inhibition of bacterial growth using antibiotics, which was much lower and ranged from 10.00 ± 1.00 mm to 10.67 ± 1.15 mm compared to the AgNPs synthesized using latex, which ranged from 10.33 ± 0.58 mm to 12.67 ± 1.15 mm, at the highest concentration (100 mg/mL). Overall, a prominent difference was noted ($p < 0.05$) for bacterial strains *E. coli*, MRSA, and *S. aureus* vs. *B. subtilis*, and all latex AgNP concentrations except 12.5 and 25 mg/mL.

Silver nanoparticles are well-known as an effective antimicrobial agent since bacteria have a weak ability to develop resistance against silver ions [5]. Previous reports have indicated that Gram-positive bacteria are usually more resistant to AgNPs due to the presence of a peptidoglycan layer that often acts as a preventive barrier for NP entry [5], compared to Gram-negative bacteria, which lacks this special layer and contains a negatively charged surface area, which attracts Ag ions, thus are more susceptible to cell membrane damage by AgNPs [57]. Similar results were observed in the present study only for the Gram-negative bacteria *E. coli* and Gram-positive bacteria *B. subtilis* and MRSA, whereas the other bacterial

strains were not consistent with previous studies [5,57]. Moreover, it was revealed that the properties of AgNPs can interact and penetrate the cell wall of bacterial cells, thus causing damage/destabilization of the outer membrane, which causes a cascade of denaturation events followed by inadequate bacterial respiration, reduced intracellular ATP, and, eventually, cell death [5,56,58–60].

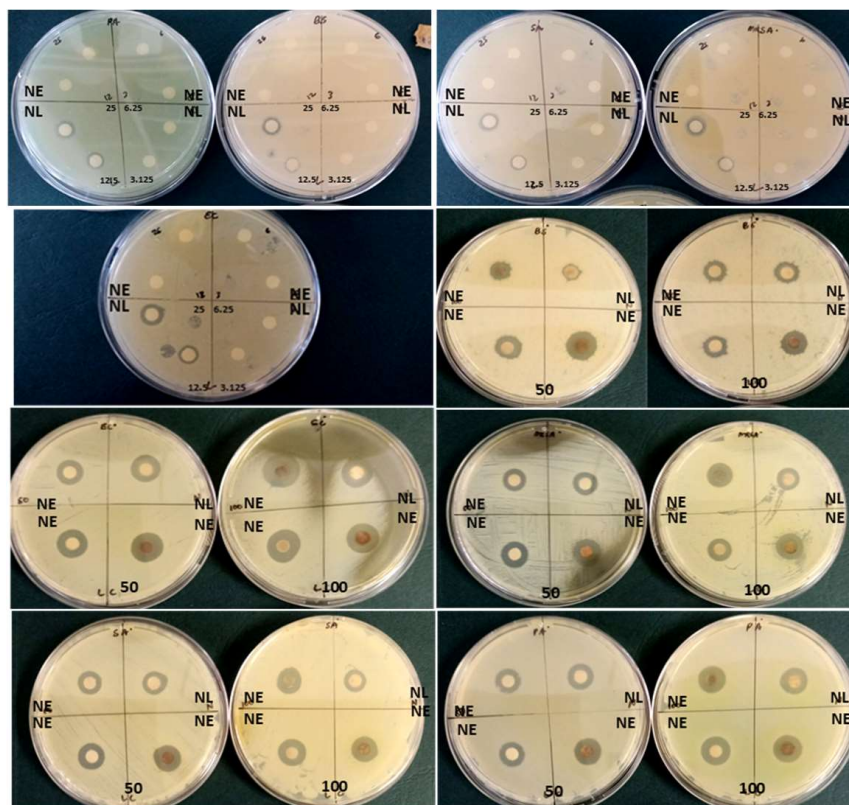


Figure 6. Diameter of zone of inhibition (mm) of nano extracts (NE) and nano latex (NL) of *T. ventricosa* at various concentrations (3.125–100 mg/mL) against Gram-positive-negative bacterial strains ($n = 3$).

3.7. Cytotoxicity Assay

Over the years, researchers have examined the cytotoxic effects of AgNPs using various plant extracts and discovered that “Green” synthesized particles exhibited inhibitory effects at low concentrations, thus deeming them safe in a variety of applications [15,49,60]. In the present study, the cytotoxicity of the AgNPs using latex extracts of *T. ventricosa* was evaluated in three human cell lines, HEK293 (embryonic kidney), MCF-7 (breast adenocarcinoma), and HeLa (cervical carcinoma). For the MTT cell viability assay (Mosmann, 1983), various concentrations of the AgNPs ranging from 15, 30, 60, 120 to 240 $\mu\text{g/mL}$ were tested. As observed in Figure 7, in positive control 1 (cells only) and control 2 (cells + 0.1% DMSO), a reduction in viability (72.56–93.12%) was noted, whereas the percentage cell survival of all cell lines was significantly reduced by biosynthesized AgNPs. As the concentration of the AgNPs increased (15, 30, 60, 120, and 240 $\mu\text{g/mL}$), the percentage of cell survival in all cell lines gradually decreased, suggesting a dose-dependent relationship. Likewise, Rajkuberan et al. [7] investigated the AgNPs using latex extracts of *Euphorbia antiquorum* L. and further assessed the in vitro cytotoxicity of the AgNPs, which similarly showed increasing anticancer activity against HeLa cells at increased concentrations. Furthermore, the results of the present study noted that at the lowest concentrations (15 $\mu\text{g/mL}$), HeLa, MCF-7, and HEK293 cells displayed moderate cytotoxicity, with HeLa cells (46.19%) displaying the most sensitivity (lowest cell survival), followed by MCF-7 (51.61%) and HEK293 (59.69%). Whereas, at the highest concentration (240 $\mu\text{g/mL}$), it was apparent that HeLa cells were

once again most sensitive, displaying significant cytotoxicity, with cell viabilities of 2.40%, followed by HEK293 (5.13%) and MCF (12.48%). Moreover, significant differences were observed for the cytotoxic analyses of latex AgNPs for all concentrations within each cell line ($p < 0.01$).

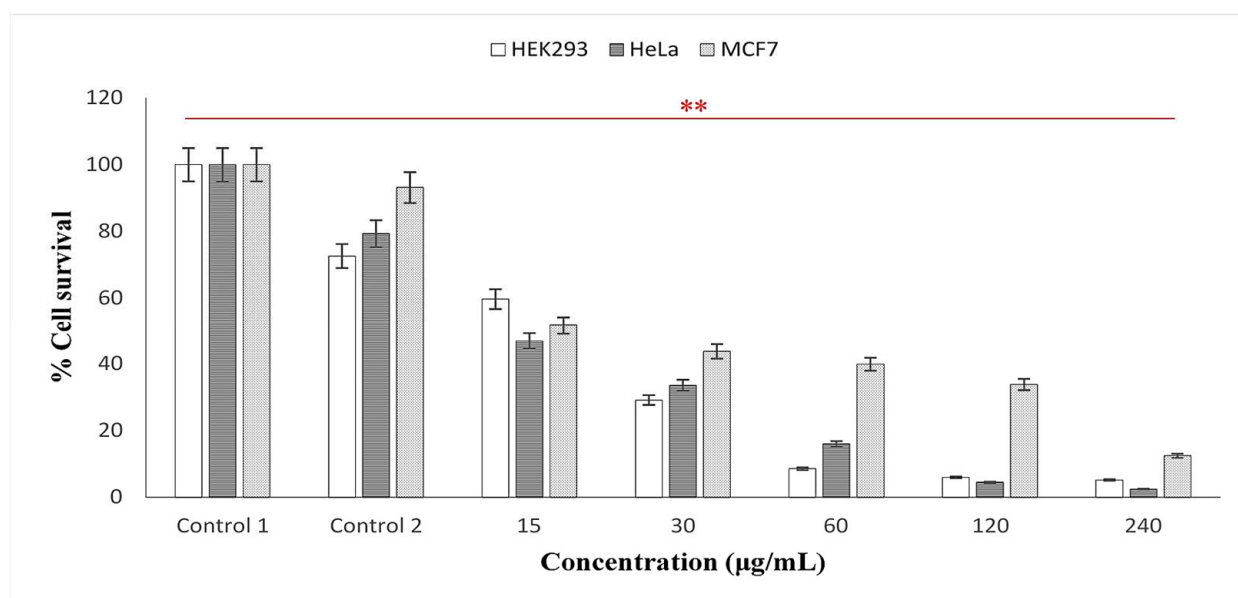


Figure 7. In vitro cytotoxicity activity of synthesized AgNPs using latex extracts from *T. ventricosa*. Control 1 = cells only; Control 2 = cells + DMSO. Percentage cell survival of HEK293; MCF-7 and HeLa cell lines. ** $p < 0.01$ is considered significant.

The IC_{50} values of latex AgNPs tested in HEK293, HeLa, and MCF-7 were 13.70 µg/mL, 10.52 µg/mL, and 20.60 µg/mL, respectively (Table 5). All IC_{50} values were suggestive of noteworthy cytotoxic activity ($IC_{50} < 50$). Across all cell lines, the most significant IC_{50} was observed for the HeLa cells. Similarly, Rajkuberan et al. [7], observed a substantial IC_{50} value (28 µg/mL) of AgNPs synthesized using *Euphorbia antiquorum* latex in the HeLa cell lines. Another report by Rajkuberan et al. [15] evaluated biosynthesized AgNPs using *Calotropis gigantea* latex against HeLa cell lines, which displayed a moderate IC_{50} of 91.30 µg/mL. These variations in the observed IC_{50} values of AgNPs synthesized using latex are possibly due to the presence of different capping compounds such as proteins and enzymes within the latex extracts [5,7,42]. It has been suggested that the mechanisms of AgNPs often induce reactive oxygen species (ROS), which damage several cellular materials such as proteins, lipids, and DNA, causing a rapid increase in oxidative stress, which ultimately activates cell death in the form of apoptosis or necrosis [7]. However, further studies are required to assess the full effects of AgNPs against the molecular mechanism on cells. This will allow us to determine possible sources of anticancer drugs.

Table 5. IC_{50} values of the cytotoxic activity of the AgNPs synthesized from the fresh latex extracts of *T. ventricosa*.

Extract	Cell Lines		
	HEK293	HeLa	MCF-7
	Concentration µg/mL		
Latex	13.70	10.52	20.60

4. Conclusions

Tabernaemontana ventricosa latex extracts were investigated in this study to effectively produce AgNPs, thus offering an environmentally friendly, cost-effective, and simple approach. The synthesized AgNPs were characterized using UV-visible spectroscopy, FTIR, SEM, HRTEM, EDX, and NTA. The antibacterial activity of AgNPs was assessed against various Gram-negative and Gram-positive bacterial strains, and the cytotoxic potential was assessed in human cell lines, namely embryonic kidney (HEK293), breast adenocarcinoma (MCF-7), and cervical carcinoma (HeLa). The AgNPs displayed prominent Ag peaks during UV-SPEC and EDX analyses. Furthermore, spherical, ovate, and triangular-shaped latex AgNPs (5.00–17.50 nm) were visible during SEM and HRTEM studies. Various functional groups within latex AgNPs, such as alcohols, alkanes, amines, proteins, enzymes, and other biomolecules, were detected by FTIR, possibly responsible for the capping, reduction, and functionalization of AgNPs. The antibacterial and cytotoxic evaluation of AgNPs displayed promising activity, thus suggesting the potential importance of AgNPs in biomedical applications. To the best of our knowledge, this is the first report on the synthesis, characterization, and antibacterial and cytotoxic evaluation of AgNPs using latex of *T. ventricosa*. Future studies will focus on latex-mediated gold and copper nanoparticles to determine an optimized size selectiveness and stability. In addition, further studies to determine the molecular mechanisms of AgNPs on cell lines will be explored.

Author Contributions: Conceptualization, C.M.N. and Y.N.; methodology, C.M.N.; validation, C.M.N., Y.N., Y.H.D., M.S. and A.A.; formal analysis, C.M.N.; investigation C.M.N., Y.N. and A.N.D.; resources, C.M.N., Y.N., M.S. and J.L.; data curation, C.M.N.; writing—original draft preparation, C.M.N.; writing—review and editing, C.M.N., Y.N., Y.H.D., M.S. and A.A.; visualization, C.M.N., Y.N., Y.H.D., M.S. and A.A. supervision Y.N., Y.H.D. and M.S.; project administration, C.M.N., Y.N., Y.H.D., M.S. and J.L. All authors have read and agreed to the published version of the manuscript.

Funding: This research was funded by the National Research Foundation, South Africa (Grant No. 131172) and Researchers Supporting Project number (RSP2023R375), King Saud University, Riyadh, Saudi Arabia.

Institutional Review Board Statement: Not applicable.

Informed Consent Statement: Not applicable.

Data Availability Statement: This study is part of C.M. Naidoo's Ph.D. thesis entitled "Micromorphological characterization, histo-phytochemical analysis and bioactivity of *Tabernaemontana ventricosa* hochst. ex a. dc. (Apocynaceae). <https://researchspace.ukzn.ac.za> (accessed on 1 August 2023).

Acknowledgments: The authors appreciatively acknowledge the Researchers Supporting Project number (RSP2023R375), King Saud University, Riyadh, Saudi Arabia. We would also like to sincerely thank the South African Medical Research Council (SAMRC) through its Division of Research Capacity Development under the Research Capacity Development Initiative. We would like to thank the Microscopy and Microanalysis Unit staff at the University of KwaZulu-Natal for their assistance with microscopy.

Conflicts of Interest: The authors declare no conflict of interest.

References

1. Mittal, A.K.; Chisti, Y.; Banerjee, U.C. Synthesis of metallic nanoparticles using plant extracts. *Biotechnol. Adv.* **2013**, *31*, 346–356. [CrossRef] [PubMed]
2. Yusuf, M. *Silver Nanoparticles: Synthesis and Applications*; Springer Nature: Cham, Switzerland, 2020.
3. Bar, H.; Bhui, D.K.R.; Sahoo, G.P.; Sarkar, P.; De, P.S.; Misra, A. Green synthesis of silver nanoparticles using latex of *Jatropha curcas*. *Colloids Surface. Physicochem. Eng. Asp.* **2009**, *339*, 134–139. [CrossRef]
4. de Matos, R.A.; da Silva Cordeiro, T.; Samad, R.E.; Vieira Jr, N.D.; Courrol, L.C. Green synthesis of stable silver nanoparticles using *Euphorbia milii* latex. *Colloids Surf. Physicochem. Eng. Asp.* **2011**, *389*, 134–137. [CrossRef]
5. Chandrasekaran, R.; Gnanasekar, S.; Seetharaman, P.; Keppanan, R.; Arockiaswamy, W.; Sivaperumal, S. Formulation of *Carica papaya* latex-functionalized silver nanoparticles for its improved antibacterial and anticancer applications. *J. Mol. Liq.* **2016**, *219*, 232–238. [CrossRef]

6. Kalaiselvi, D.; Mohankumar, A.; Shanmugam, G.; Nivitha, S.; Sundararaj, P. Green synthesis of silver nanoparticles using latex extract of *Euphorbia tirucalli*: A novel approach for the management of root knot nematode, *Meloidogyne incognita*. *Crop Prot.* **2019**, *117*, 108–114. [\[CrossRef\]](#)
7. Rajkuberan, C.; Prabukumar, S.; Sathishkumar, G.; Wilson, A.; Ravindran, K.; Sivaramakrishnan, S. Facile synthesis of silver nanoparticles using *Euphorbia antiquorum* L. latex extract and evaluation of their biomedical perspectives as anticancer agents. *J. Saudi Chem. Soc.* **2017**, *21*, 911–919. [\[CrossRef\]](#)
8. Masurkar, S.A.; Chaudhari, P.R.; Shidore, V.B.; Kamble, S.P. Rapid biosynthesis of silver nanoparticles using *Cymbopogon citratus* (lemongrass) and its antimicrobial activity. *Nano-Micro Lett.* **2011**, *3*, 189–194. [\[CrossRef\]](#)
9. Anbukkarasi, M.; Thomas, P.A.; Sheu, J.R.; Geraldine, P. In vitro antioxidant and anticataractogenic potential of silver nanoparticles biosynthesized using an ethanolic extract of *Tabernaemontana divaricata* leaves. *Biomed. Pharmacother.* **2017**, *91*, 467–475. [\[CrossRef\]](#)
10. Anbukkarasi, M.; Thomas, P.A.; Teresa, P.A.; Anand, T.; Geraldine, P. Comparison of the efficacy of a *Tabernaemontana divaricata* extract and of biosynthesized silver nanoparticles in preventing cataract formation in an in-vivo system of selenite-induced cataractogenesis. *Biocatal. Agric. Biotechnol.* **2020**, *23*, 101475. [\[CrossRef\]](#)
11. Manasa, D.J.; Chandrashekar, K.R.; Kumar, P.; Suresh, D.; Madhu Kumar, D.J.; Ravikumar, C.R.; Bhattacharya, T.; Murthy, H.C. Proficient Synthesis of Zinc Oxide Nanoparticles from *Tabernaemontana Heyneana* Wall. Via Green Combustion Method: Antioxidant, Anti-Inflammatory, Antidiabetic, Anticancer and Photocatalytic Activities. *Results Chem.* **2021**, *3*, 100178. [\[CrossRef\]](#)
12. Salem, W.M.; Haridy, M.; Sayed, W.F.; Hassan, N.H. Antibacterial activity of silver nanoparticles synthesized from latex and leaf extract of *Ficus sycomorus*. *Ind. Crop. Prod.* **2014**, *62*, 228–234. [\[CrossRef\]](#)
13. Valodkar, M.; Jadeja, R.N.; Thounaojam, M.C.; Devkar, R.V.; Thakore, S. In vitro toxicity study of plant latex-capped silver nanoparticles in human lung carcinoma cells. *Mater. Sci. Eng.* **2011**, *31*, 1723–1728. [\[CrossRef\]](#)
14. Guidelli, E.J.; Ramos, A.P.; Zaniquelli, M.E.D.; Baffa, O. Green synthesis of colloidal silver nanoparticles using natural rubber latex extracted from *Hevea brasiliensis*. *Spectrochim. Acta A Mol. Biomol. Spectrosc.* **2011**, *82*, 140–145. [\[CrossRef\]](#) [\[PubMed\]](#)
15. Rajkuberan, C.; Sudha, K.; Sathishkumar, G.; Sivaramakrishnan, S. Antibacterial and cytotoxic potential of silver nanoparticles synthesized using latex of *Calotropis gigantea* L. *Spectrochim. Acta A Mol. Biomol. Spectrosc.* **2015**, *136*, 924–930. [\[CrossRef\]](#)
16. Schmidt, E.; Lotter, M.; McClelland, W. *Trees and Shrubs of Mpumalanga and Kruger National Park*; Jacana Media: Johannesburg, South Africa, 2002; pp. 566–569.
17. Schmelzer, G.B.; Gurib-Fakim, A. Plant Resources of Tropical Africa (PROTA). In *Medicinal Plants*, 1st ed.; Backhuys Publishers: Wageningen, The Netherlands, 2008; Volume 1, pp. 597–598.
18. Mehrbod, P.; Abdalla, M.A.; Njoya, E.M.; Ahmed, A.S.; Fotouhi, F.; Farahmand, B.; Gado, D.A.; Tabatabaian, M.; Fasanmi, O.G.; Eloff, J.N.; et al. South African medicinal plant extracts active against influenza A virus. *BMC Complement. Altern. Med.* **2018**, *18*, 112–121. [\[CrossRef\]](#)
19. Van Beek, T.; Deelder, A.; Verpoorte, R.; Svendsen, A. Antimicrobial, Antiamoebic and Antiviral Screening of some *Tabernaemontana* Species. *Planta Med.* **1984**, *50*, 180–185. [\[CrossRef\]](#)
20. Andima, M.; Ndakala, A.; Derese, S.; Biswajyoti, S.; Hussain, A.; Yang, L.J.; Akoth, O.E.; Coghi, P.; Pal, C.; Heydenreich, M.; et al. Antileishmanial and cytotoxic activity of secondary metabolites from *Tabernaemontana ventricosa* and two aloe species. *Nat. Prod. Res.* **2021**, *36*, 1365–1369. [\[CrossRef\]](#)
21. Schripsema, J.; Hermans-Lokkerbol, A.; Van Der Heijden, R.; Verpoorte, R.; Svendsen, A.B.; Van Beek, T.A. Alkaloids of *Tabernaemontana ventricosa*. *J. Nat. Prod.* **1986**, *49*, 733–735. [\[CrossRef\]](#)
22. Ambu, G.; Chaudhary, R.P.; Mariotti, M.; Cornara, L. Traditional uses of medicinal plants by ethnic people in the Kavrepalanchok district, Central Nepal. *Plants* **2020**, *9*, 759. [\[CrossRef\]](#)
23. Chandra, H.; Kumar, P.; Bontempi, E.; Yadav, S. Medicinal plants: Treasure trove for green synthesis of metallic nanoparticles and their biomedical applications. *Biocatal. Agric. Biotechnol.* **2020**, *24*, 101518. [\[CrossRef\]](#)
24. Clinical and Laboratory Standards Institute (CLSI). *Performance Standards for Antimicrobial Disk Susceptibility Tests*; Wayne, P.A., Ed.; Clinical and Laboratory Standards Institute (CLSI): Wayne, PA, USA, 2006.
25. Marathe, N.P.; Rasane, M.H.; Kumar, H.; Patwardhan, A.A.; Shouche, Y.S.; Diwanay, S.S. In vitro antibacterial activity of *Tabernaemontana alternifolia* (Roxb) stem bark aqueous extracts against clinical isolates of methicillin resistant *Staphylococcus aureus*. *Ann. Clin. Microbiol. Antimicrob.* **2013**, *12*, 26. [\[CrossRef\]](#) [\[PubMed\]](#)
26. Mosmann, T. Rapid colorimetric assay for cellular growth and survival: Application to proliferation and cytotoxicity assays. *J. Immunol. Methods.* **1983**, *65*, 55–63. [\[CrossRef\]](#) [\[PubMed\]](#)
27. Daniels, A.N.; Singh, M. Sterically stabilized siRNA: Gold nanocomplexes enhance c-MYC silencing in a breast cancer cell model. *Nanomedicine* **2019**, *14*, 1387–1401. [\[CrossRef\]](#) [\[PubMed\]](#)
28. Rathnayake, I.; Ismail, H.; Azahari, B.; De Silva, C.; Darsanasiri, N. Imparting antimicrobial properties to natural rubber latex foam via green synthesized silver nanoparticles. *J. Appl. Polym. Sci.* **2014**, *131*, 1–10. [\[CrossRef\]](#)
29. Kumar, V.; Yadav, S.K. Plant-mediated synthesis of silver and gold nanoparticles and their applications. *J. Chem. Technol. Biotechnol.* **2009**, *84*, 151–157. [\[CrossRef\]](#)
30. Lee, K.X.; Shameli, K.; Yew, Y.P.; Teow, S.Y.; Jahangirian, H.; Rafiee-Moghaddam, R.; Webster, T.J. Recent developments in the facile bio-synthesis of gold nanoparticles (AuNPs) and their biomedical applications. *Int. J. Nanomed.* **2020**, *15*, 275. [\[CrossRef\]](#)

31. Zargar, M.; Hamid, A.A.; Bakar, F.A.; Shamsudin, M.N.; Shameli, K.; Jahanshiri, F.; Farahani, F. Green synthesis and anti-bacterial effect of silver nanoparticles using *Vitex negundo* L. *Molecules* **2011**, *16*, 6667–6676. [\[CrossRef\]](#)
32. Akula, R.; Ravishankar, G.A. Influence of abiotic stress signals on secondary metabolites in plants. *Plant Sigant. Behav.* **2011**, *6*, 1720–1731. [\[CrossRef\]](#)
33. Sigamoney, M.; Shaik, S.; Govender, P.; Krishna, S.B.N. African leafy vegetables as bio-factories for silver nanoparticles: A case study on *Amaranthus dubius* C Mart. Ex Thell. *S. Afr. J. Bot.* **2016**, *103*, 230–240. [\[CrossRef\]](#)
34. Hu, S.; Hsieh, Y.L. Silver nanoparticle synthesis using lignin as reducing and capping agents: A kinetic and mechanistic study. *Int. J. Biol. Macromol.* **2016**, *82*, 856–862. [\[CrossRef\]](#)
35. Almeida, L.M.; Magno, L.N.; Pereira, A.C.; Guidelli, É.J.; Baffa Filho, O.; Kinoshita, A.; Goncalves, P.J. Toxicity of silver nanoparticles released by *Hancornia speciosa* (Mangabeira) Biomembrane. *Spectrochim. Acta A Mol. Biomol. Spectrosc.* **2019**, *210*, 329–334. [\[CrossRef\]](#) [\[PubMed\]](#)
36. Akwu, N.A.; Naidoo, Y.; Singh, M.; Nundkumar, N.; Daniels, A.; Lin, J. Two Temperatures Biogenic Synthesis of Silver Nanoparticles from *Grewia lasiocarpa* E. Mey. ex Harv. Leaf and Stem Bark Extracts: Characterization and Applications. *J. BioNano Sci.* **2021**, *11*, 142–158. [\[CrossRef\]](#)
37. Sathishkumar, M.; Sneha, K.; Won, S.W.; Cho, C.W.; Kim, S.; Yun, Y.S. Cinnamon zeylanicum bark extract and powder mediated green synthesis of nano-crystalline silver particles and its bactericidal activity. *Colloids Surf. B* **2009**, *73*, 332–338. [\[CrossRef\]](#) [\[PubMed\]](#)
38. Patil, C.D.; Borase, H.P.; Patil, S.V.; Salunkhe, R.B.; Salunke, B.K. Larvicidal activity of silver nanoparticles synthesized using *Pergularia daemia* plant latex against *Aedes aegypti* and *Anopheles stephensi* and nontarget fish *Poecilia reticulata*. *Parasitol. Res.* **2012**, *111*, 555–562. [\[CrossRef\]](#) [\[PubMed\]](#)
39. Borase, H.P.; Patil, C.D.; Suryawanshi, R.K.; Patil, S.V. *Ficus carica* latex-mediated synthesis of silver nanoparticles and its application as a chemophotoprotective agent. *Appl. Biochem. Biotechnol.* **2013**, *171*, 676–688. [\[CrossRef\]](#)
40. Song, J.Y.; Jang, H.K.; Kim, B.S. Biological synthesis of gold nanoparticles using *Magnolia kobus* and *Diopyros kaki* leaf extracts. *Process Biochem.* **2009**, *44*, 1133–1138. [\[CrossRef\]](#)
41. Yaqoob, A.A.; Umar, K.; Ibrahim, M.N.M. Silver nanoparticles: Various methods of synthesis, size affecting factors and their potential applications—a review. *Appl. Nanosci.* **2020**, *10*, 1369–1378. [\[CrossRef\]](#)
42. Durgawale, P.P.; Phatak, R.S.; Hendre, A.S. Biosynthesis of silver nanoparticles using latex of *Syandanium grantii* Hook f and its assessment of antibacterial activities. *Dig. J. Nanomater. Bios.* **2015**, *10*, 847.
43. Magudapathy, P.; Gangopadhyay, P.; Panigrahi, B.K.; Nair, K.G.M.; Dhara, S. Electrical transport studies of Ag nanoclusters embedded in glass matrix. *Physica B Condens. Matter* **2001**, *299*, 142–146. [\[CrossRef\]](#)
44. Annadurai, G.; Gnanajobitha, G.; Kannan, C. Green synthesis of silver nanoparticle using *Elettaria cardamomom* and assessment of its anti-microbial activity. *Int. J. Pharm. Sci.* **2021**, *3*, 323–330.
45. Devaraj, P.; Aarti, C.; Kumari, P. Synthesis and characterization of silver nanoparticles using *Tabernaemontana divaricata* and its cytotoxic activity against MCF7 cell line. *Int. J. Pharmacol. Pharm. Sci.* **2014**, *6*, 86–90.
46. Bakar, N.A.; Ismail, J.; Bakar, M.A. Synthesis and characterization of silver nanoparticles in natural rubber. *Mater. Chem. Phys.* **2007**, *104*, 276–283. [\[CrossRef\]](#)
47. Raheman, F.; Deshmukh, S.; Ingle, A.; Gade, A.; Rai, M. Silver nanoparticles: Novel antimicrobial agent synthesized from an endophytic fungus *Pestalotia* sp. isolated from leaves of *Syzygium cumini* (L). *Nano Biomed. Eng.* **2011**, *3*, 174–178. [\[CrossRef\]](#)
48. Banu, A.; Rathod, V. Synthesis and characterization of silver nanoparticles by *Rhizopus stolonier*. *Int. J. Biomed. Adv. Res.* **2011**, *2*, 148–158. [\[CrossRef\]](#)
49. Mohamed, N.H.; Ismail, M.A.; Abdel-Mageed, W.M.; Shoreit, A.A.M. Antimicrobial activity of latex silver nanoparticles using *Calotropis procera*. *Asian Pac. J. Trop. Biomed.* **2014**, *4*, 876–883. [\[CrossRef\]](#)
50. Mohamed, N.H.; Ismail, M.A.; Abdel-Mageed, W.M.; Shoreit, A.A.M. Antimicrobial activity of green silver nanoparticles from endophytic fungi isolated from *Calotropis procera* (Ait) latex. *Microbiology* **2019**, *165*, 967–975. [\[CrossRef\]](#) [\[PubMed\]](#)
51. Akinyelu, J.; Singh, M. Folate-tagged chitosan functionalized gold nanoparticles for enhanced delivery of 5-fluorouracil to cancer cells. *Appl. Nanosci.* **2019**, *9*, 7–17. [\[CrossRef\]](#)
52. Oladimeji, O.; Akinyelu, J.; Daniels, A.; Singh, M. Modified Gold Nanoparticles for efficient Delivery of Betulinic Acid to Cancer Cell Mitochondria. *Int. J. Mol. Sci.* **2021**, *22*, 5072. [\[CrossRef\]](#)
53. Kumar, V.; Yadav, S.C.; Yadav, S.K. *Syzygium cumini* leaf and seed extract mediated biosynthesis of silver nanoparticles and their characterization. *J. Chem. Technol. Biotechnol.* **2010**, *85*, 1301–1309. [\[CrossRef\]](#)
54. Fatima, K.; Mahmud, S.; Yasin, H.; Asif, R.; Qadeer, K.; Ahmad, I. Authentication of various commercially available crude drugs using different quality control testing parameters. *Pak. J. Pharm. Sci.* **2020**, *33*, 1641–1657.
55. Preetam Raj, J.P.; Purushothaman, M.; Ameer, K.; Panicker, S.G. In-vitro anticancer and antioxidant activity of gold nanoparticles conjugate with *Tabernaemontana divaricata* flower SMs against MCF-7 breast cancer cells. *Korean Chem. Eng. Res.* **2016**, *54*, 5–80. [\[CrossRef\]](#)
56. Attri, P.; Garg, S.; Ratan, J.K.; Giri, A.S. Silver Nanoparticles from *Tabernaemontana Divaricate* leaf extract: Mechanism of action and Bio-application for photo degradation of 4-Aminopyridine. *Res. Sq.* **2021**, *30*, 24856–24875. [\[CrossRef\]](#) [\[PubMed\]](#)
57. Shrivastava, S.; Bera, T.; Roy, A.; Singh, G.; Ramachandrarao, P.; Dash, D. Characterization of enhanced antibacterial effects of novel silver nanoparticles. *Nanotechnology* **2007**, *18*, 225103. [\[CrossRef\]](#) [\[PubMed\]](#)

58. Vivekanandhan, S.; Christensen, L.; Misra, M.; Mohanty, A.K. Biosynthesis of silver nanoparticles using *murraya koenigii* (curry leaf): An investigation on the effect of broth concentration in reduction mechanism and particle size. *Adv. Mater. Lett.* **2011**, *2*, 429–434.
59. Raja, A.; Ashokkumar, S.; Marthandam, R.P.; Jayachandiran, J.; Khatiwada, C.P.; Kaviyarasu, K.; Raman, R.G.; Swaminathan, M. Eco-friendly preparation of zinc oxide nanoparticles using *Tabernaemontana divaricata* and its photocatalytic and antimicrobial activity. *J. Photochem. Photobiol. Biol.* **2018**, *181*, 53–58. [[CrossRef](#)]
60. Hassan, M.H.; Ismail, M.A.; Moharram, A.M.; Shoreit, A.A. Phytochemical and antimicrobial of latex serum of *Calotropis procera* and its silver nanoparticles against some reference pathogenic strains. *J. Ecol. Health Environ.* **2017**, *5*, 65–75. [[CrossRef](#)]

Disclaimer/Publisher's Note: The statements, opinions and data contained in all publications are solely those of the individual author(s) and contributor(s) and not of MDPI and/or the editor(s). MDPI and/or the editor(s) disclaim responsibility for any injury to people or property resulting from any ideas, methods, instructions or products referred to in the content.